

# OBSERVED CHANGES IN THE SIERRA NEVADA SNOWPACK: POTENTIAL CAUSES AND CONCERNS

*A Report From:*  
**California Climate Change Center**

*Prepared By:*  
**Sarah Kapnick and Alex Hall**

## DISCLAIMER

This paper was prepared as the result of work sponsored by the California Energy Commission (Energy Commission) and the California Environmental Protection Agency (Cal/EPA). It does not necessarily represent the views of the Energy Commission, Cal/EPA, their employees, or the State of California. The Energy Commission, Cal/EPA, the State of California, their employees, contractors, and subcontractors make no warrant, express or implied, and assume no legal liability for the information in this paper; nor does any party represent that the uses of this information will not infringe upon privately owned rights. This paper has not been approved or disapproved by the California Energy Commission or Cal/EPA, nor has the California Energy Commission or Cal/EPA passed upon the accuracy or adequacy of the information in this paper.



*Arnold Schwarzenegger, Governor*



**DRAFT PAPER**

March 2009  
CEC-500-2009-016-D



## Acknowledgments

Sarah Kapnick is supported by a National Aeronautics and Space Administration (NASA) Earth and Space Science Fellowship (#07-Earth07F-0232) and a Jet Propulsion Laboratory (JPL) fellowship entitled: "Earth Climate Science: Collaborative Investigations with UCLA Graduate Students" (#1313181). Alex Hall is supported by University of California Water Resources grant WR1024. The writers would also like to gratefully acknowledge funding provided by JPL (#1312546) under a project entitled: "Evaluating key uncertainties in IPCC Climate Change projection of California snowpack: Topography, snow, physics and aerosol deposition."



## Preface

The California Energy Commission's Public Interest Energy Research (PIER) Program supports public interest energy research and development that will help improve the quality of life in California by bringing environmentally safe, affordable, and reliable energy services and products to the marketplace.

The PIER Program conducts public interest research, development, and demonstration (RD&D) projects to benefit California's electricity and natural gas ratepayers. The PIER Program strives to conduct the most promising public interest energy research by partnering with RD&D entities, including individuals, businesses, utilities, and public or private research institutions.

PIER funding efforts focus on the following RD&D program areas:

- Buildings End-Use Energy Efficiency
- Energy-Related Environmental Research
- Energy Systems Integration
- Environmentally Preferred Advanced Generation
- Industrial/ Agricultural/ Water End-Use Energy Efficiency
- Renewable Energy Technologies
- Transportation

In 2003, the California Energy Commission's PIER Program established the **California Climate Change Center** to document climate change research relevant to the states. This center is a virtual organization with core research activities at Scripps Institution of Oceanography and the University of California, Berkeley, complemented by efforts at other research institutions. Priority research areas defined in PIER's five-year Climate Change Research Plan are: monitoring, analysis, and modeling of climate; analysis of options to reduce greenhouse gas emissions; assessment of physical impacts and of adaptation strategies; and analysis of the economic consequences of both climate change impacts and the efforts designed to reduce emissions.

**The California Climate Change Center Report Series** details ongoing center-sponsored research. As interim project results, the information contained in these reports may change; authors should be contacted for the most recent project results. By providing ready access to this timely research, the center seeks to inform the public and expand dissemination of climate change information, thereby leveraging collaborative efforts and increasing the benefits of this research to California's citizens, environment, and economy.

For more information on the PIER Program, please visit the Energy Commission's website [www.energy.ca.gov/pier/](http://www.energy.ca.gov/pier/) or contract the Energy Commission at (916) 654-5164.



## Table of Contents

Preface.....	iii
Abstract.....	vii
1.0 Introduction.....	1
2.0 Data.....	2
3.0 Methods and Results.....	3
3.1. Calculation of Snow Mass Peak.....	3
3.2. Trends in Peak Snow Mass Timing.....	5
3.3. Distribution of Peak Snow Mass Timing Versus April 1 SWE.....	7
3.4. Relationships Between Peak Snow Mass Timing and Temperature.....	9
4.0 Summary.....	12
5.0 Discussion.....	12
6.0 References.....	13
 Appendix Test of Snow Course Cohesiveness.....	 A-1

## List of Figures

- Figure 1. Locations of 352 snow stations with usable data in the California. Open circles denote Natural Resources Conservation Service (NRCS) Water and Climate Center stations and closed circles denote California Department of Water Resources for California stations. Stations are colored by elevation in meters.....3
- Figure 2. The blue line denotes daily 1996 SWE values at the SNOTEL Adin Mtn station from January 1 to May 31. The red bars represent the approximated SWE values used to calculate the peak snow mass timing from February 1 to May 1. The red hatch on each bar denotes the first of February, March, April, and May. The dashed line at Julian Day 72.09 denotes the SCD found by this method.....4
- Figure 3. SCD for 27 stations with annual data available for at least 75% of the record from 1930 to 2007. There are 1,778 data points for the time period. The dashed line denotes the mean SCD (Julian day 76.8) and the solid line denotes the linear trendline for the time series.....5
- Figure 4. Trend in SCD versus trend in April 1 SWE for 27 stations with at least 75% of years available from 1930 to 2007. Stations are the same ones used for Figure 3. Dashed lines denote trends of zero. Stations are colored by elevation in meters. Circled stations have statistically significant trends (at  $p < 0.1$ ) in April 1 SWE and/or SCD. ....7

Figure 5. Scatterplot of SCD versus April 1 SWE value for 61 stations with at least 75% of years available from 1948 to 2007, colored by the monthly mean local March temperature. Temperature data are given in degrees Celsius and is from the NCEP Reanalysis 1 monthly mean surface temperature data set (available from 1948 to 2007) and has been adjusted for station elevation assuming a constant lapse rate of 6.5°C per kilometer (km) or 18.8°F per mile (mi). If the graph is confined to stations with 75% of years available from 1930 to 2007, a similar distribution is found. Changing the start date of the plot does not materially affect the distribution of SCD versus April 1 SWE values. The average SCD for the data set is Julian day 75.4, and is given by the dashed black line.....8

Figure 6. Scatterplot of March Sierra temperature versus SCD for 61 stations from 1948 to 2007 for: (a) observations of SCD and modeled local temperature, (b) anomalies, and (c) mean values. The dashed red line denotes the linear trendline on each graph. The two variables are strongly anti-correlated for all plots: (a)  $r = -0.38$ , (b)  $r = -0.41$ , and (c)  $r = -0.44$ , with  $p < 0.01$  for all graphs. If the correlation is calculated for the variables when they are detrended, the anti-correlations are not materially different..... 10

## List of Tables

Table 1. Trend in peak timing (days per decade) from start date (denoted in columns) to 2007 for three different cases: all stations with available SCD data, stations with data for only 50% of available years, and stations with data for only 75% of available years. The trend corresponding to Figure 3 is given by the highlighted cell. The last row provides the average March surface temperature trend (°C per decade) found in the gridcells covering the snow stations.....5

## Abstract

A study of the California Sierra snowpack has been conducted using snow station observations and reanalysis surface temperature data. First-of-the-month snow water equivalent measurements were combined from two data sets to provide sufficient data from 1930 to 2007. The monthly snapshots are used to calculate peak snow mass timing for each snow season. Since 1930, there has been a trend toward earlier snow mass peak timing by 0.4 days per decade. The trend towards earlier timing also occurs at most individual stations. The majority of stations have experienced simultaneous reductions in April 1 snow water equivalent. Reductions in April 1 snow water equivalent may therefore be due to earlier snowmelt rather than reductions in total snowfall. Analysis of individual years and stations reveals that warm March temperatures are associated with earlier snow mass peak timing for all spatial and temporal scales included in the data set. The influence is particularly pronounced for low accumulation years indicating the importance of albedo feedback for the melting of shallow snow. Regional mean March temperatures have increased at a rate of 0.4°C or 1.8°F per decade since 1948, and the robustness of the March temperature influence on peak timing suggests the trend towards earlier peak timing is attributable to the March temperature trend. Given scenarios of warming in California, we can expect to see acceleration in the peak timing trend; this will reduce the warm season storage capacity of the California snowpack.

**Keywords:** Snowpack, peak, snow water equivalent, snowmelt, water supply, climate change, warming



## 1.0 Introduction

The California water supply is determined primarily by cold season precipitation (rain in low elevations and snow in high elevations) and the capacity of natural and man-made reservoirs. Most man-made reservoirs were built in the early twentieth century and designed under the assumption that they would be filled during initial cold season rains. This water would then be used during cold months, depleting reservoirs until replenished during the warm season by mountain snowmelt. By the end of the summer and early fall, the reservoirs would again reach a minimum before being refilled by the next cold season precipitation. Thus, reservoirs were designed to store only a fraction of the state's entire yearly precipitation, under the assumption that the annual mountain snowpack would melt at roughly the same time every year. During anomalously high rain or snowmelt events, reservoirs must not only store water, but also discharge excess water to avoid flooding. Water must sometimes be discharged in anticipation of large events to reduce flood risk. The dual functions of storage and flood management require reservoir managers to carefully balance factors such as precipitation, snowmelt timing, reservoir storage capacity, and demand. Even if future precipitation remains unchanged, shifts in snowmelt timing can affect California's water supply during the warm season due to reservoir storage capacity constraints. To understand changes in snowmelt water supply as a result of climate change, it is therefore important to understand changes in the timing of snowmelt in addition to spring snowpack values.

Snowpack measurements are essential for predicting timing and amount of warm season snowmelt runoff. For this reason, a network of stations in the western United States dating back to the 1930s tracks water content of snow (also known as snow water equivalent, or *SWE*). Measurements are taken manually around the first of the month at each station according to a prescribed monthly schedule. Because of the desire to track peak *SWE*—thought to occur in early April—many more records are available for dates on or around April 1 (Serreze et al. 1999). Previous snowpack studies have focused on this well-sampled April 1 *SWE* data set to assess the relationship between climatology and variability of snowpack in the western United States (Barnett et al. 2008; Mote et al. 2005; Cayan 1996). These studies are important for understanding total melt water available during the warm months, but do not directly address accumulation and melt events occurring earlier in the season.

Ideally, high-temporal resolution data would be available to study the evolution of the snowpack over the course of the season; particularly data that would reveal the exact date of maximum *SWE* and subsequent melt rates. Stations have been built in California since the 1970s to measure daily *SWE* automatically, but the period of record for these sites is not long enough for long-term variability analysis. Previous observational studies have instead utilized streamflow data, presumably snowmelt-dominated, as a proxy for snowmelt timing. Using a variety of streamflow metrics they show there has been a trend in streamflow discharge toward earlier in the spring (Regonda et al. 2005; Stewart et al. 2005; Cayan et al. 2001). Daily *SWE* data from 1992 to 2002 have also been combined with long-term historic streamflow data to study the onset of spring in the Sierra Nevada (Lundquist et al. 2004); however, because of the shortness of the *SWE* time series, streamflow measurements must still be relied upon to measure long-term variability in snowmelt. Unfortunately, streamflow is indirectly related to snowmelt, making it an imperfect proxy for snowmelt, as it can be influenced by other factors such as

precipitation, temperature, lithology, soil composition, vegetation (Aguado et al. 1992), and pre-snowmelt soil moisture.

To study changes in the California snowpack directly, the present study focuses on monthly SWE data. A data set has been compiled from two different sources to provide sufficient stations with SWE measurements for February 1 through May 1 over a long enough time period to do robust trend analysis. The monthly data are used to infer peak snow mass timing from February to May. Over this record stretching roughly from 1930 to the present, the peak timing exhibits a trend toward earlier in the season. This trend can be explained by the sensitivity of snow mass peak timing to local March temperature. Given future warming scenarios in the California Sierra Nevada, we conclude the trend in earlier peak timing will continue.

## 2.0 Data

A snow station data set for the State of California was compiled from two existing data sets: the National Resources Conservation Service and Water and Climate Center ([www.wcc.nrcs.usda.gov/snowcourse/](http://www.wcc.nrcs.usda.gov/snowcourse/)) and the California Department of Water Resources (<http://cdec.water.ca.gov/misc/SnowCourses.html>). A total of 352 stations across California recorded SWE data for at least 15 years from 1930 to 2007 (see Figure 1). These stations range in their months and years of available data. We address the impact of temporal gaps on our analysis in Appendix A. Subsequent sections will describe criteria used to produce subsets of data for analysis.

Temperature data are also used to diagnose snow accumulation and melt processes. Surface temperature data from 1948 to 2007 were obtained from the National Centers for Environmental Prediction/National Center for Atmospheric Research (NCEP/NCAR) Reanalysis 1 data set (Kalnay et al. 1996) provided by the NOAA/OAR/ESRL PSD,<sup>1</sup> Boulder, Colorado ([www.cdc.noaa.gov](http://www.cdc.noaa.gov)). This data set was chosen for its long temporal coverage and high (2.5 degree) spatial resolution relative to other pre-satellite era temperature products.

---

<sup>1</sup> National Oceanic and Atmospheric/Office of Oceanic and Atmospheric Research/Earth System Research Laboratory Physical Science Division

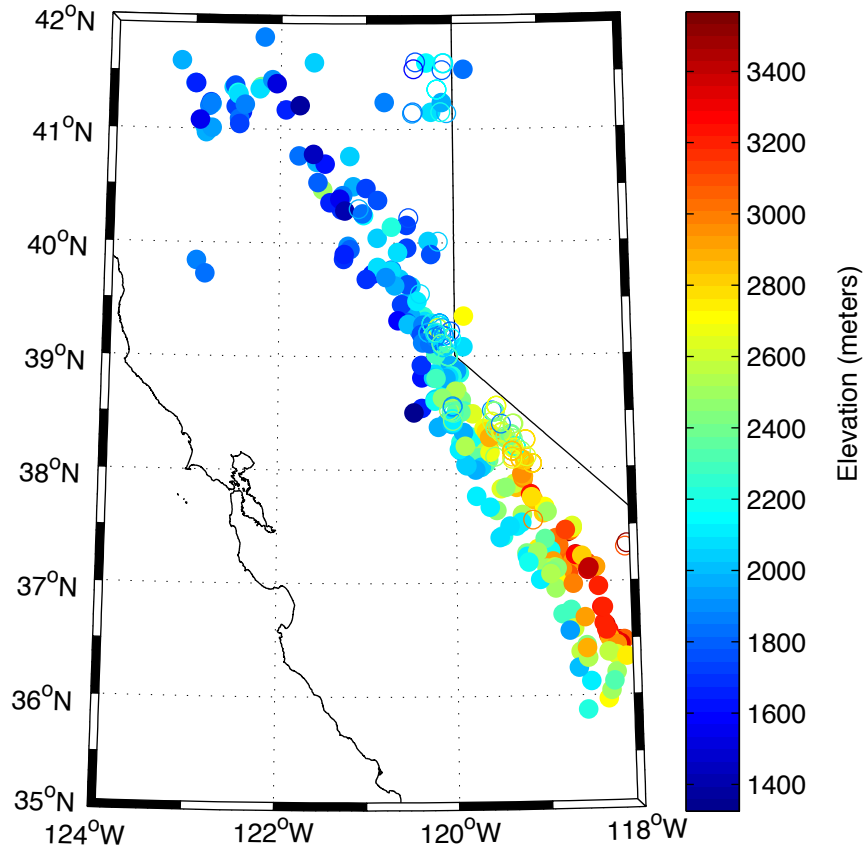


**Figure 1. Locations of 352 snow stations with usable data in the California. Open circles denote Natural Resources Conservation Service (NRCS) Water and Climate Center stations and closed circles denote California Department of Water Resources for California stations. Stations are colored by elevation in meters.**

### 3.0 Methods and Results

#### 3.1. Calculation of Snow Mass Peak

To assess inter-annual variations in California snowpack evolution, a metric was developed for quantifying systematic changes in snow accumulation and melt timing. In particular, we focused on the timing of peak snow mass. We created a measure of the timing of peak snow mass relying on first-of-the-month SWE values from February to May. We used these monthly snapshots rather than daily SWE data because the daily data are only robustly available from 1980 to the present, too short a time series to calculate long-term trends in maximum SWE timing.

The peak snow mass timing is defined for any given year as the temporal centroid date, also known as the center of mass, of SWE values (SWE centroid date, or *SCD*) from February 1 to May 1 for stations with complete data over this four-month time period. The *SCD* is given by the equation:

$$SCD = \frac{\sum t_i SWE_i}{\sum SWE_i}$$

Each individual measurement from February 1 to May 1 is distinguished by  $i$ . The first-of-the-month SWE measurements, given by  $SWE_i$  in centimeters (cm), are assumed to represent the average SWE values for the halves of the months preceding and following the measurement dates (i.e., a midpoint approximation was taken for each month). The value  $t_i$  represents time covered by each measurement in days. There are four such intervals from the middle of January to the middle of May. The SCD metric is similar to that used in previous studies of streamflow peak timing (Stewart et al. 2005; Stewart et al. 2004). Figure 2 provides a visualization of this calculation for a location and a year for which daily data are also available. As is clear from the figure, this metric captures the gross timing of snow processes. For the peak to shift earlier (later), the percentage of snow accumulation later in the season must decrease (increase), or there must be an increase (decrease) in the percentage of snow melting later in the season. Thus it corresponds roughly with the peak in snow mass.

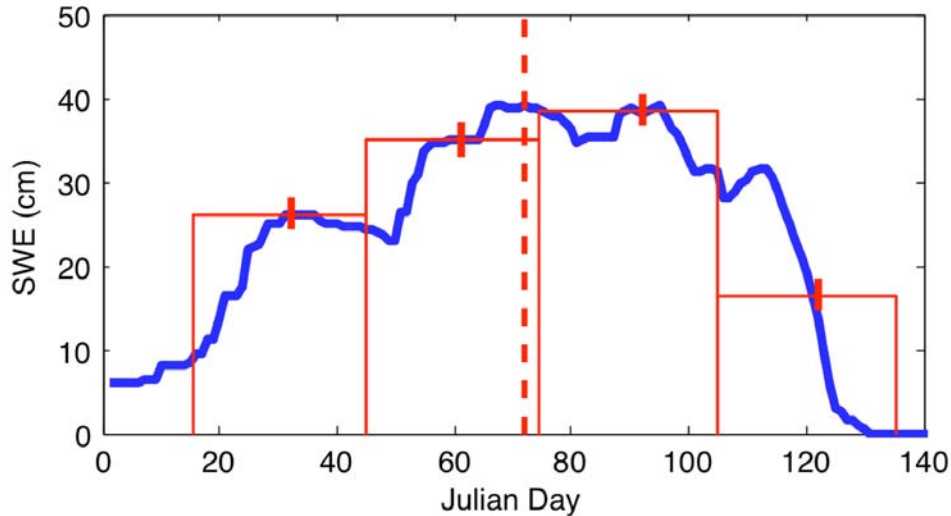


**Figure 2. The blue line denotes daily 1996 SWE values at the SNOTEL Adin Mtn station from January 1 to May 31. The red bars represent the approximated SWE values used to calculate the peak snow mass timing from February 1 to May 1. The red hatch on each bar denotes the first of February, March, April, and May. The dashed line at Julian Day 72.09 denotes the SCD found by this method.**

The SCD metric provides a more accurate representation of the timing of snow accumulation and melt than the date of the absolute maximum SWE value given in the four first-of-the-month point measurements. It allows for the snow mass peak timing to shift on the order of days instead of being constrained to shifts in monthly increments. Long-term variability in snow mass peak timing can be studied on sub-month time scales despite the lack of daily data. As we show below, the changes in peak snow mass timing in the Sierra are order days, confirming the need for a metric with this property.

### 3.2. Trends in Peak Snow Mass Timing

Examination of SCD from 1930 to 2007 yields evidence that it is trending earlier. When stations with data for at least 75% of these years are included, SCD is found to occur earlier at a rate of 0.4 days per decade (Figure 3). This is similar to figures showing trends in earlier spring timing in Cayan et al. (2001). In a given year, there is a spread in SCD between the data points, mainly due to the spatial and altitudinal variability of the set of stations. The yearly average SCD for the set of stations also fluctuates according to the seasonal variability in SCD caused by seasonal differences in accumulation and melt. Over the SCD record however, there is an overall trend in SCD for the set of stations used. This trendline has a slope significantly different than zero (using the Student's T-test,  $p < 0.01$ ). When stations with fewer yearly SCD values are also included, or when the starting year of the trendline is set later to include more stations, statistically significant trendlines of earlier peak timing are still found (Table 1). In most cases, the trend towards earlier peak timing is enhanced (i.e., the trend becomes more negative). There is a similar enhancement in the March temperature warming trend from 1950 to 1970 as successively later periods of the time series are isolated (Table 1). We discuss the potential causal link between the warming and SCD trends in the discussion.

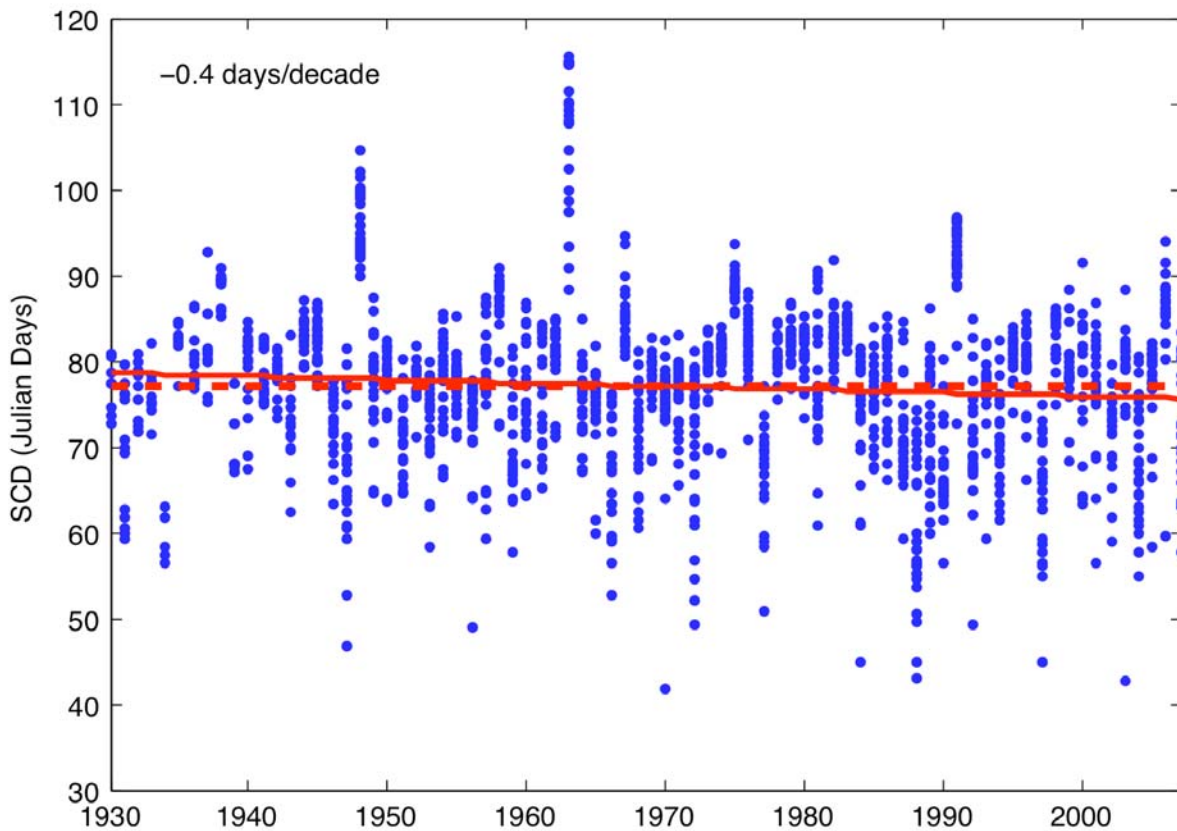


Figure 3. SCD for 27 stations with annual data available for at least 75% of the record from 1930 to 2007. There are 1,778 data points for the time period. The dashed line denotes the mean SCD (Julian day 76.8) and the solid line denotes the linear trendline for the time series.

Table 1. Trend in peak timing (days per decade) from start date (denoted in columns) to 2007 for three different cases: all stations with available SCD data, stations with

**data for only 50% of available years, and stations with data for only 75% of available years. The trend corresponding to Figure 3 is given by the highlighted cell. The last row provides the average March surface temperature trend (°C per decade) found in the gridcells covering the snow stations.**

Case	1930	1940	1950	1960	1970
All Stations	-0.4	-0.5	-0.3	-0.5	-0.5
50% of Years	-0.6	-0.7	-0.4	-0.7	-0.7
75% of Years	-0.4	-0.6	-0.6	-0.7	-0.6
March Temperature	-	-	0.3	0.5	0.7

Almost all individual station SCD trends are also negative (Figure 4), suggesting a consistent signal from catchment to catchment. Figure 4 compares station trends in SCD to trends in the highly-studied April 1 SWE record, finding that 24 of the 27 stations have negative trends in SCD from 1930 to 2007. The majority of stations exhibit a negative trend in both SCD and April 1 SWE (17 out of 27 stations). The only stations exhibiting statistically significant trends in SCD and April 1 SWE also have negative trends in both metrics (2 stations). A negative SCD trend is likely caused by snow melting earlier, resulting in less April 1 SWE. This hypothesis will be explored in Section 3.4. A long-term reduction in seasonal accumulation could also affect SCD. The relationship between accumulation (measured by April 1 SWE) and SCD is discussed in Section 3.3. The points in Figure 4 with positive trends in April 1 SWE but negative trends in SCD all have positive trends in SWE from February to May (not shown). This suggests there has been a large enough increase in snowfall at these locations to offset whatever additional loss is occurring due to enhanced late-season melting.

These results show that examining historic April 1 SWE trends alone may be misleading as a metric of the Sierra Nevada snowpack trends. A minor decrease in April 1 SWE values at some stations may be due to the shift in SCD—a reflection of increased snowmelt before April 1—rather than a reduction in total snowfall at the station. This phenomenon has been observed in some daily Snowpack Telemetry (*SNOTEL*) stations in the Sierra; April 1 SWE was shown to be highly anti-correlated with daily melt events from the previous months, implying changes in April 1 SWE have been due at least in part to melt events (Mote et al. 2005). For stations with positive April 1 SWE trends coupled with negative SCD trends, April 1 SWE may similarly be too low an estimate of the snowfall increase.

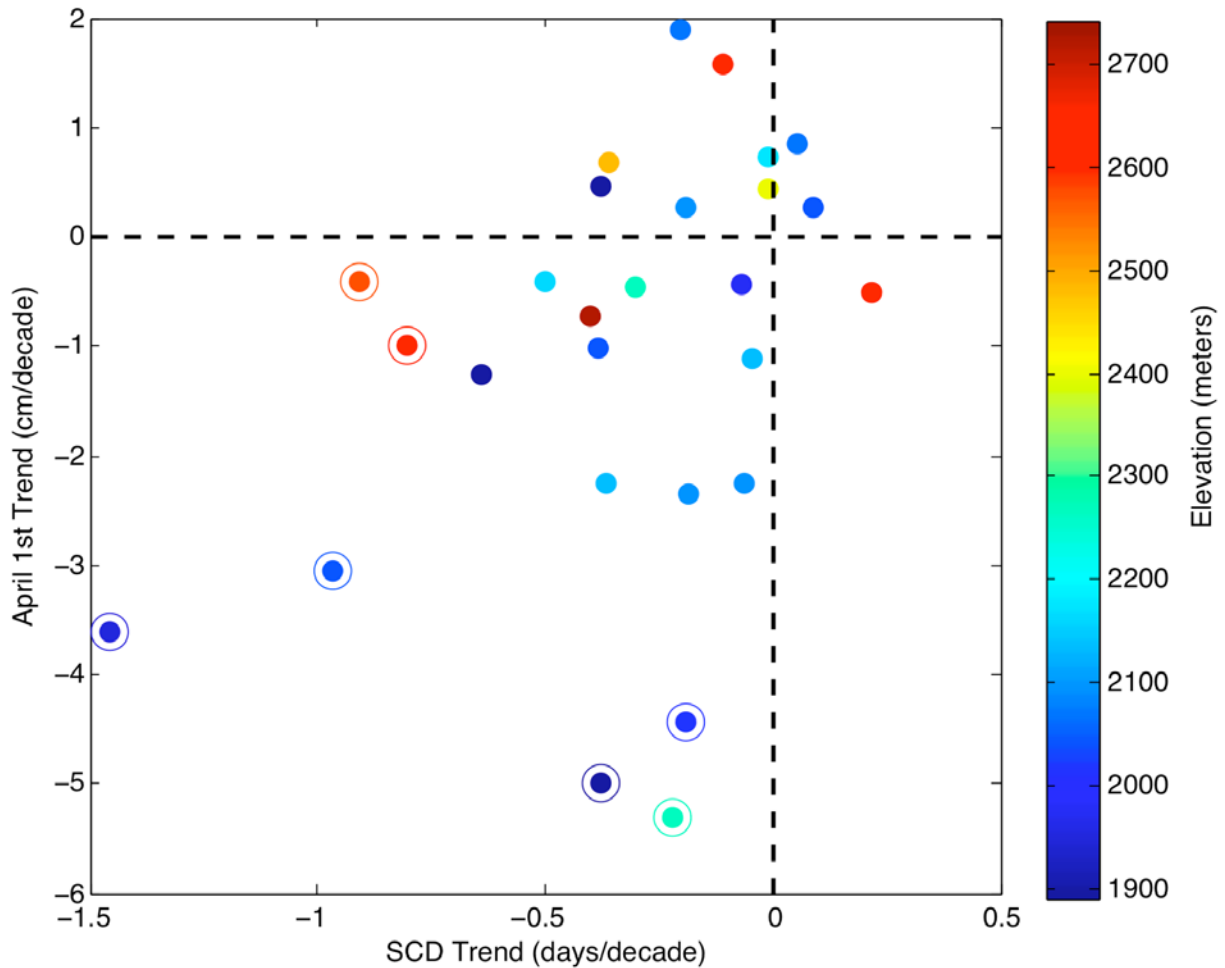


**Figure 4.** Trend in SCD versus trend in April 1 SWE for 27 stations with at least 75% of years available from 1930 to 2007. Stations are the same ones used for Figure 3. Dashed lines denote trends of zero. Stations are colored by elevation in meters. Circled stations have statistically significant trends (at  $p < 0.1$ ) in April 1 SWE and/or SCD.

### 3.3. Distribution of Peak Snow Mass Timing Versus April 1 SWE

Variability in April 1 SWE is evaluated against variability in the SCD metric to explore relationships between SCD and the SWE variable used to predict water supply. Figure 5 shows a scatterplot of April 1 SWE versus SCD values. Each point represents a snow station during one snow season. Snow stations with a minimum of 75% of SCD values over the period from 1948 to 2007 were used for this analysis. This time period was selected to coincide with the available temperature record. (A nearly identical distribution is found if the start date is changed to 1930.) For the given subset of snow stations, SCD occurs over a wide range, with the average SCD occurring on Julian day 75.4 (mid March). The average April 1 SWE value is 76.4 cm (30.1 inches).

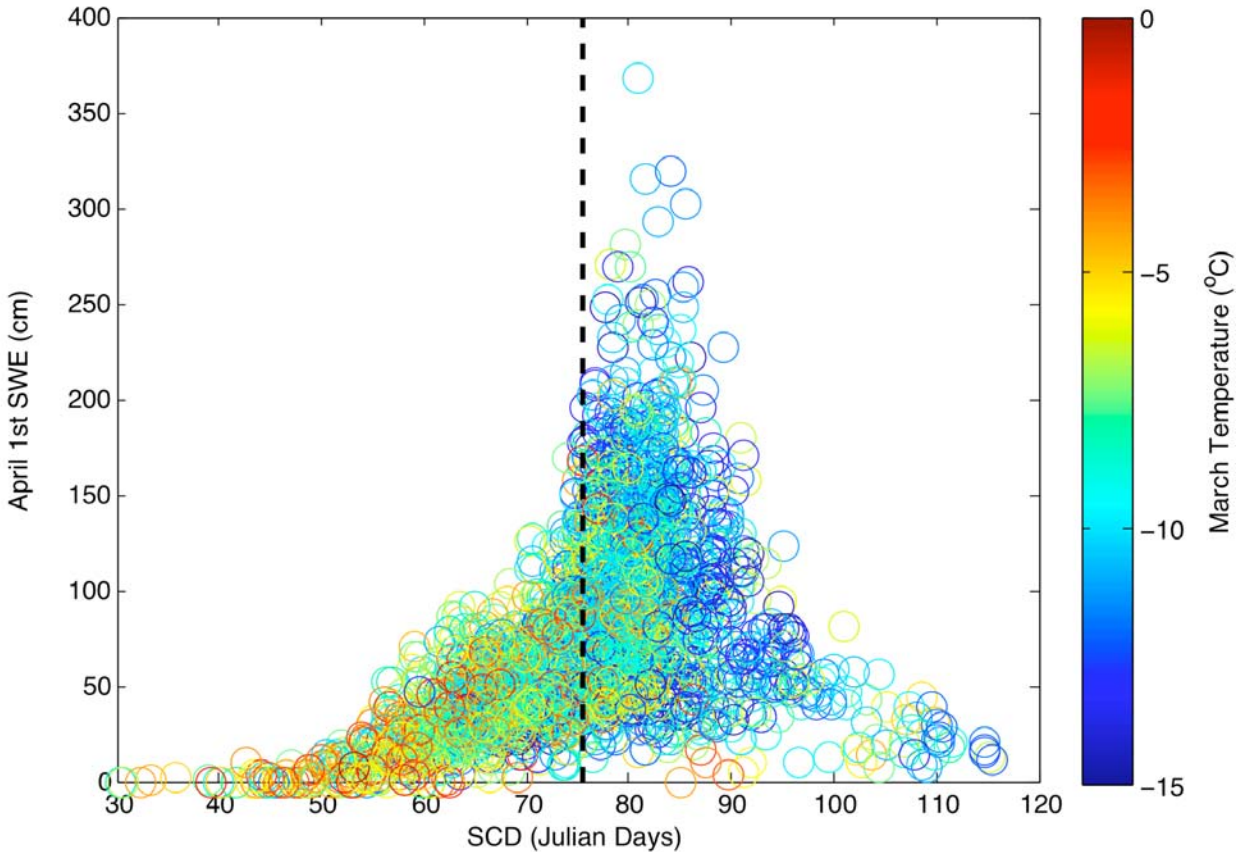


**Figure 5. Scatterplot of SCD versus April 1 SWE value for 61 stations with at least 75% of years available from 1948 to 2007, colored by the monthly mean local March temperature. Temperature data are given in degrees Celsius and is from the NCEP Reanalysis 1 monthly mean surface temperature data set (available from 1948 to 2007) and has been adjusted for station elevation assuming a constant lapse rate of 6.5°C per kilometer (km) or 18.8°F per mile (mi). If the graph is confined to stations with 75% of years available from 1930 to 2007, a similar distribution is found. Changing the start date of the plot does not materially affect the distribution of SCD versus April 1 SWE values. The average SCD for the data set is Julian day 75.4, and is given by the dashed black line.**

The striking bell-shaped distribution of the April 1 SWE versus SCD scatterplot arises because of differing behavior of SCD for large and small seasonal snow accumulation. When April 1 SWE is large (roughly greater than or equal to 100 cm or 39.4 inches), the SCD tends to occur in a narrow band between Julian day 68 and 95, with most points (93%) above the mean of 75.4. This corresponds to a time period mainly falling between the middle of the second and third bar of Figure 2, or the calendar month of March. There are three main reasons for this behavior:

1. To attain such high April 1 SWE values, relatively consistent storm activity and steady accumulation is necessary during the duration of the snow season.
2. The large accumulation then increases the effective thermal inertia of the snowpack, delaying the onset of melting in the lower layers of the snow column and eventual disappearance of the snowpack.
3. This large accumulation then only melts once the seasonal warming becomes great enough to initiate the melting process.

These three processes make for a late SCD, with little variation from season to season.

When April 1 SWE is small (less than roughly 100 cm) however, the SCD falls over a large range between Julian day 30 and 116. This range is more than three times that of the high seasonal accumulation and covers the middle of the first bar to the middle of the fourth bar in Figure 2, or from the last day in January to the end of April. The significantly greater range in SCD values is due to two factors:

1. Low accumulation is the result of a relatively small number of storms with highly variable timing.
2. Melting in shallow snow is more sensitive to temperatures above freezing because of the smaller thermal inertia of shallow snow and its greater susceptibility to albedo feedback. This results in earlier (later) snowmelt when temperatures are warm (cold).

To explore the sensitivity of SCD to temperature further, the colorbar given in Figure 5 distinguishes the distribution of SCD values by local monthly March temperature. The local monthly average temperature for each station is calculated by taking the local gridbox surface temperature and adjusting it for elevation assuming a constant lapse rate of  $6.5^{\circ}\text{C}/\text{km}$  ( $18.8^{\circ}\text{F}/\text{mi}$ ). When the distribution of SCD versus April 1 SWE is distinguished by temperature, SCD has very little systematic association with either January or February temperatures (not shown), but is closely linked to March temperatures. Lower March temperatures appear to shift SCD into the later half of the season. The most likely reason for this connection is that snowmelt between March and April is increased (reduced) by anomalously warm (cold) March temperatures, thus moving SCD to the later (earlier) portion of the season. The sensitivity to March temperature is particularly pronounced for years when April 1 SWE is low, providing direct evidence of the greater susceptibility of shallow snow to albedo feedback.

### **3.4. Relationships Between Peak Snow Mass Timing and Temperature**

Figure 5 provides visual evidence that air temperature, the primary thermodynamic control of melt, is potentially a major variable affecting SCD. Figure 6a provides a statistical measure the link between March temperature and SCD for the entire data set. March temperature is found to shift SCD earlier in the season by 1.3 days per degree Celsius (0.7 days per degree Fahrenheit), and is significantly anti-correlated ( $r = -0.38$ ,  $p < 0.01$ ) with SCD. As noted in Section 3.2, the trend towards earlier SCD coincides with a trend toward warmer March temperature. The anti-correlation between SCD and March temperature seen in Figure 6a could result from these two trends. However, when the SCD and temperature time series are detrended, the anti-correlation is very similar (-0.40). This suggests the link between March temperatures and SCD is robust for variability as well as trends in SCD, a point we return to in the discussion.

Figures 6b and 6c further examine the SCD-March temperature relationship when controlled for spatial and temporal variability. In Figure 6b, the temporal SCD and March temperature anomalies (defined as the observation value minus the mean value at each station) are compared. Here we eliminate any systematic relationship between SCD and March temperature in Figure 6a arising from the fact that the stations are at different locations and therefore have different climatological temperatures. Conversely, in Figure 6c, temporal variability is eliminated by comparing station mean SCD values against station mean March temperatures. Thus, each

point on the graph is an individual station. A negative relationship between SCD and March temperature remains when spatial and temporal variability are each isolated in turn. This provides evidence of the predictive value of March temperature for both spatial and temporal variability in SCD.

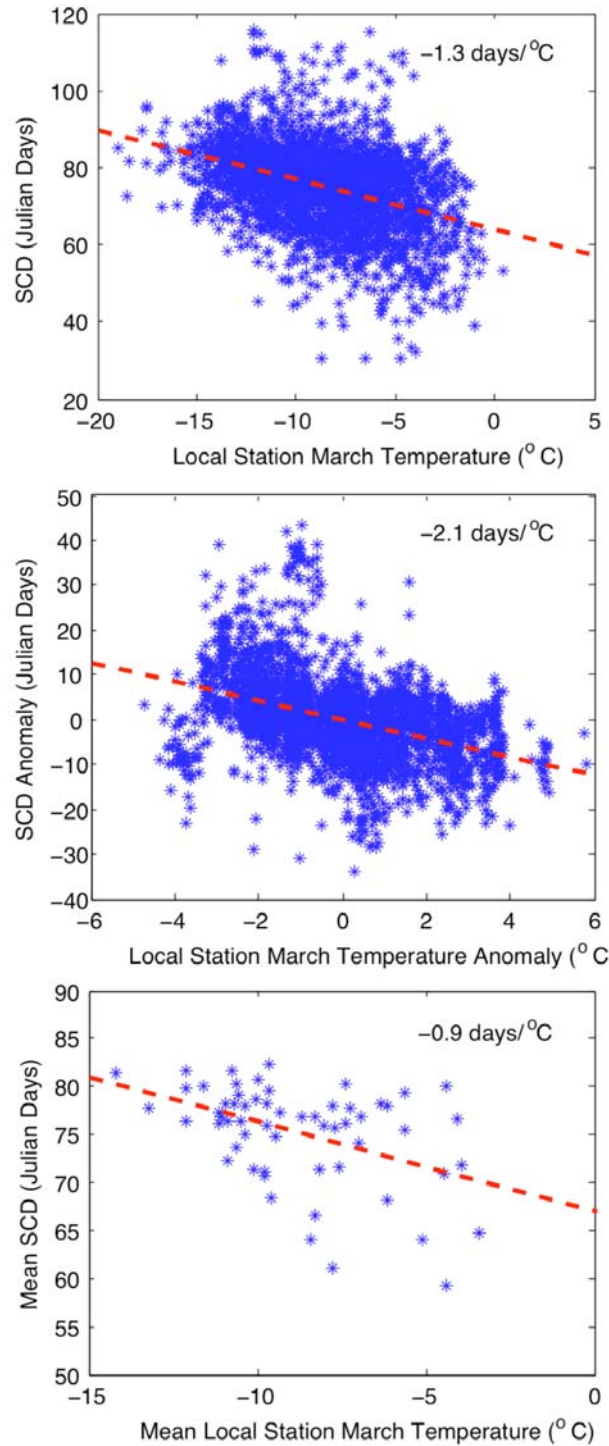


**Figure 6. Scatterplot of March Sierra temperature versus SCD for 61 stations from 1948 to 2007 for: (a) observations of SCD and modeled**

local temperature, (b) anomalies, and (c) mean values. The dashed red line denotes the linear trendline on each graph. The two variables are strongly anti-correlated for all plots: (a)  $r = -0.38$ , (b)  $r = -0.41$ , and (c)  $r = -0.44$ , with  $p < 0.01$  for all graphs. If the correlation is calculated for the variables when they are detrended, the anti-correlations are not materially different.

## 4.0 Summary

In this study, a metric is developed to calculate peak snow mass timing in the California Sierra Mountains using monthly SWE data from 1930 to 2007. Robust statistical analysis is conducted to assess the variability in the timing of peak snow mass. From 1930 to present, the peak timing of the entire data set exhibits a trend towards earlier in the season of 0.4 days per decade. On an individual station basis, most stations show earlier SCD and reduced April 1 SWE, and the only stations with statistically significant trends in both SCD and April 1 SWE exhibit negative trends in both variables. The trends in SCD complicate interpretations of April 1 SWE as a metric of Sierra Nevada snowpack trends. The influence of March temperature on SCD is almost certainly due to the effect of March temperature on snowmelt. This relationship is particularly evident for low accumulation years, indicating the importance of albedo feedback for the melting of shallow snow. The robustness in the sensitivity of SCD to March temperature for all spatial and temporal scales included in the data set indicates the SCD trend can be attributed to the March warming trend.

The trend in snow mass peak timing found in this study is less than those of snowmelt-dominated streamflow found in previous studies (Regonda et al. 2005; Stewart et al. 2005; Cayan et al. 2001), which provide changes in the date of peak runoff on the order of a few days per decade. These order of magnitude differences in the trends in these metrics may be accounted for by the fact that a shift in the timing of streamflow runoff is not necessarily accompanied by an equal shift in peak snow mass due to differences in the calculation of streamflow metrics and SCD. In fact, if the shift in SCD is due to earlier snowmelt, the snowmelt acceleration would probably have to be much more rapid than the SCD shift. This is due to the steadiness of the weights of the accumulation months (i.e. February 1, March 1) in the SCD calculation. The involvement of four months of data in the SCD calculation introduces more “inertia” into this quantity than streamflow pulse onset (a measure of snowmelt runoff). The time period of study and stream gauges used in streamflow studies also do not necessarily match up precisely with the snow stations used in this present study. Further study of the link between changes in snowmelt and streamflow is necessary to elucidate the mechanisms affecting California water supply.

## 5.0 Discussion

Taken together, this study and previous studies paint a picture of a California Sierra snowpack responding rapidly to the changing climate of the past few decades. These trends are likely to continue. Extrapolating the current trend in March temperatures, peak snow mass timing should continue to occur earlier. Projections of temperature in California in the coming decades show that the trend in annual temperature may accelerate, with surface temperatures increasing by 2°C (3.6°F) to 7°C (12.6°F) by 2100 (Cayan et al. 2008). Assuming a similar distribution of temperature changes in March, we can calculate a projection of the shift in SCD by the end of the century. Using the relationship between temperature and SCD anomalies in Figure 6b, this implies a shift in the SCD from current mean values by 4 to 14 days earlier by the end of the century, with potentially much larger shifts in snowmelt timing if recent relationships between the two variables are any guide. Comparing regression calculations of trends in SCD and March temperature provides additional confidence that the sensitivity of SCD to March temperature is accurate. From 1948 to 2007, there has been a trend in SCD and March temperature of -0.8

days per decade and 0.4°C per decade (0.7°F per decade), respectively. This corresponds to a calculated SCD sensitivity to March temperature of roughly -2 days per degree Celsius (1.1 days per degree Fahrenheit), the value given by Figure 6b and found by regression.

These extrapolations into the future may be too conservative because the trends in SCD found in this study are probably low estimates of future changes in peak snow mass timing. This is because snow season temperatures will rise above the freezing point with increasing frequency as the climate continues to warm, leading to more precipitation falling as rain instead of snow. By and large, this threshold has not been reached on average for March yet. In the analysis in Figure 6, there is only one instance in the record since 1948 of the local station average March temperature being above 0°C (32°F). Thus, most stations currently exhibit snow accumulation between March 1 and April 1. As temperatures begin to rise above the critical threshold of 0°C (32°F) much more often during March, melt rates will continue increasing, but precipitation will also shift from being dominated by snow to rain, eventually resulting in net melt rather than accumulation from March 1 to April 1. Stations at lower elevations will be the first to exhibit this change in accumulation dynamics. As the shift to rain will also impact SWE values in the latest part of the season first, it will contribute to the advance of SCD. The calculated sensitivity of SCD to March temperatures does not reflect this mechanism yet, and therefore is probably a lower bound.

In this study, SWE observations have directly shown that the Sierra Nevada snowpack has been melting earlier in the year than it did in the past and that this trend will likely continue and accelerate in the future. Given the importance of high-resolution streamflow predictions for state water supply and reservoir management purposes, continued research on the California Sierra Nevada snowpack, a significant source of warm-season streamflow, is critical to understanding the state's future water supply. Continuation of SWE measurements is necessary to monitor and predict changes in the water supply from the Sierra Nevada snowpack. Regional modeling studies of the Sierra would also be helpful to determine the mechanisms affecting accumulation and melt events and to identify regions where precipitation will shift from being snow-dominated to rain-dominated. Future work should focus on determining which water basins will be the first to be materially affected by shifts in snowmelt timing. This information will help water managers determine necessary infrastructure changes to handle major shifts in the timing of spring runoff. An understanding of the mechanisms affecting the snowpack and streamflow runoff is necessary to help predict the future of the California water supply.

## 6.0 References

- Aguado, E., D. Cayan, L. Riddle, and M. Roos. 1992. "Climatic Fluctuations and the Timing of West Coast Streamflow." *Journal of Climate* 5:1468–1483.
- Barnett, T., D. Pierce, H. Hidalgo, C. Bonfils, B. Santer, T. Das, G. Bala, A. Wood, T. Nozawa, A. Mirin, D. Cayan, and M. Dettinger. 2008. "Human-Induced Changes in the Hydrology of the Western United States." *Science Express* 10.1126/science.1152538.
- Cayan, D. 1996. "Interannual Climate Variability and Snowpack in the Western United States." *Journal of Climate* 9: 928–948.

- Cayan, D., S. Kammerdiener, M. Dettinger, J. Caprio, and D. Peterson. 2001. "Changes in the Onset of Spring in the Western United States." *Bulletin of American Meteorological Society* 82: 339–415.
- Cayan, D., E. Maurer, M. Dettinger, M. Tyree, and K. Hayhoe. 2008. "Climate change scenarios for the California region." *Climatic Change* 87(S1): 21–42.
- Kalnay, E., M. Kanamitsu, R. Kistler, W. Collins, D. Deaven, L. Gandin, M. Iredell, S. Saha, G. White, J. Woollen, Y. Zhu, M. Chelliah, W. Ebisuzaki, W. Higgins, J. Janowiak, K. Mo, C. Ropelewski, J. Wang, A. Leetmaa, R. Reynolds, R. Jenne, and D. Joseph. 1996. "The NCEP/NCAR 40-year Reanalysis Project." *Bulletin of American Meteorological Society* 77: 437–470.
- Lundquist, J., D. Cayan, and M. Dettinger. 2004. "Spring Onset in the Sierra Nevada: When is Snowmelt Independent of Elevation?" *Journal of Hydrometeorology* 5: 327–342.
- Mote, P., A. Hamlet, M. Clark, and D. Lettenmaier. 2005. "Declining Mountain Snowpack in Western North America." *Bulletin of American Meteorological Society* 86: 39–49.
- Regonda, S., B. Rajagopalan, M. Clark, and J. Pitlick. 2005. "Seasonal cycle shifts in hydroclimatology over the western United States." *Journal of Climate* 18: 372–384.
- Serreze, M., M. Clark, R. Armstrong, D. McGinnis, and R. Pulwarty. 1999. "Characteristics of the western United States snowpack from snowpack telemetry (SNOTEL) data." *Water Resources Research* 35: 2145–2160.
- Stewart, I., D. Cayan, and M. Dettinger. 2004. "Changes in Snowmelt Runoff Timing in Western North America under a 'Business as Usual' Climate Change Scenario." *Climatic Change* 62: 217–232.
- Stewart, I., D. Cayan, and M. Dettinger. 2005. "Changes toward earlier streamflow timing across Western North America." *Journal of Climate* 18: 1136–1155.

## **Appendix**

### **Test of Snow Station Cohesiveness**

## Appendix

### Test of Snow Station Cohesiveness

If stations exhibit different accumulation patterns—entirely possible given their broad geographical and altitudinal distribution—they must be treated as subgroups of data rather than as a single system to avoid overgeneralization of the behavior of the snowpack.

Understanding the spatial variability of SWE is therefore a necessary step in our study. To achieve this, we calculate the spatial coherence of the first of the month SWE values. The subset of stations for each month (February, March, April, and May) with yearly values available for 75% of the time period from 1930 to 2007 is used for this analysis. For each month, the time series of SWE values averaged over the state are calculated and then correlated with each individual station time series. The results are then plotted in Figure A-1.

We find that snow stations are generally highly spatially correlated with the mean SWE value for the snowpack, especially those stations below 40° N. For example, in the month of April, 208 stations have correlations to the mean SWE value above 0.70 with  $p < 0.05$ . This pattern persists from February 1 to May 1, implying SWE anomalies are fairly uniform across the state for all months. The overall spatial coherence of snowpack variability demonstrates that minor temporal gaps at individual stations will not materially affect analysis of the climatology and variability of the overall California snowpack when the data set is taken as a cohesive group. This finding is especially important for the trend analysis found in Section 3.2 and shown in Figure 3 as some stations do not have data over the entire time period of interest (1930 to 2007). Sensitivity analysis of calculated trends are also provided when stations with different temporal records are used (Table 1).

It should be noted that the station below 40° N with the lowest correlation to the mean SWE time series is also the station with the lowest elevation. This location likely has different meteorological conditions, temperature patterns, and may experience snowmelt earlier and more frequently throughout the snow accumulation season than points at higher elevation. Because of its aberrant behavior, this station is left out of other analyses conducted in this study.

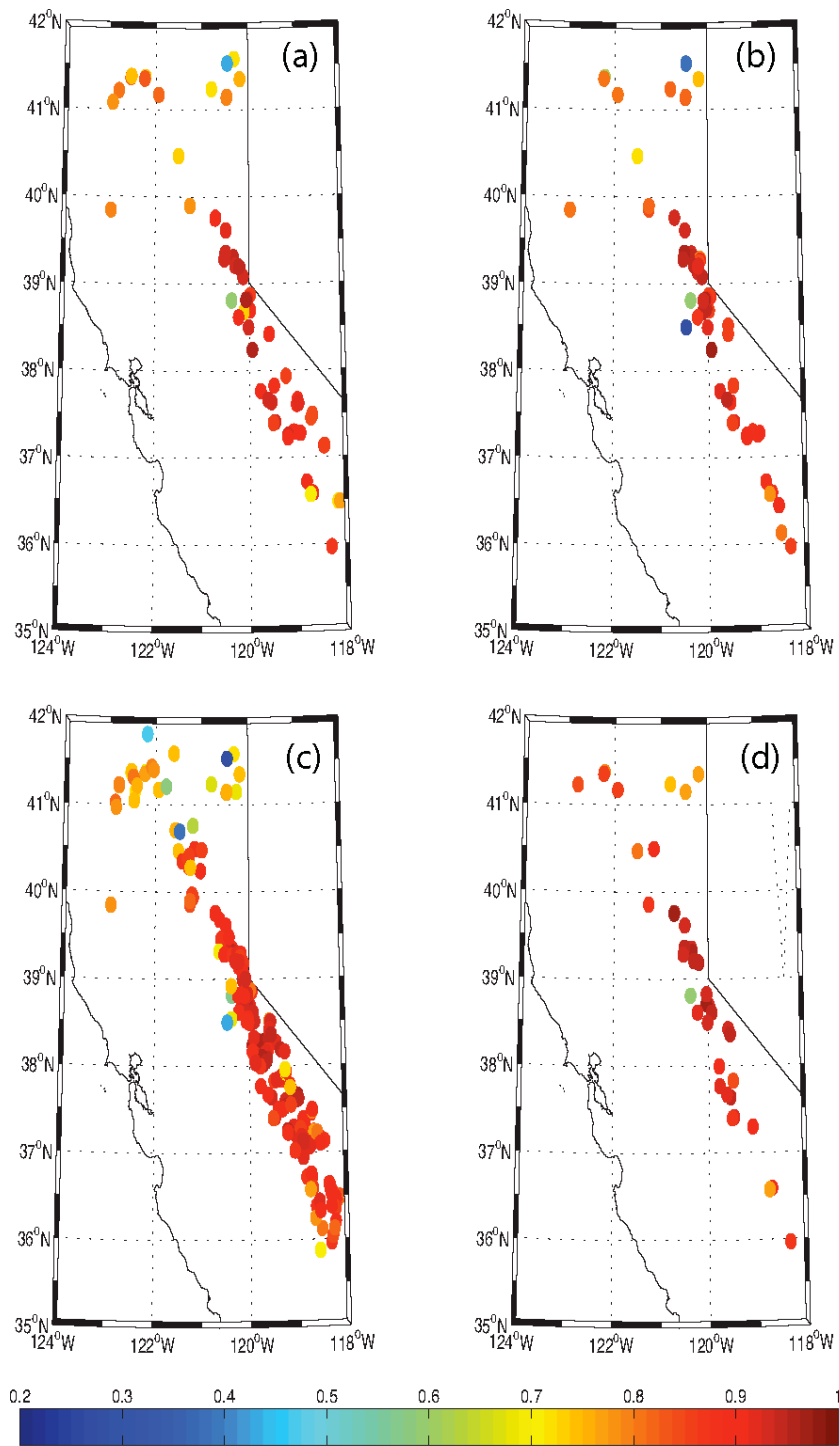


**Figure A-1. Correlation of individual station data versus collective station yearly mean SWE. Only stations with data for 75% of yearly data between 1930 and 2007 are used. Correlations are calculated on a first-of-the-month basis for (a) February, (b) March, (c) April, and (d) May. There were respectively 66, 62, 218, and 43 stations in each month.**